

# Network Pharmacology and Experimental Analysis to Explore the Effect and Mechanism of Modified Buyang Huanwu Decoction in the Treatment of Diabetic Nephropathy

Fan Yang<sup>1,\*</sup>, Limin Pan<sup>2,\*</sup>, Xiaoyun Zhang<sup>1,\*</sup>, Jiaan Huang<sup>3</sup>, Yan Liu<sup>3</sup>, Peixuan Li<sup>3</sup>, Yuehua Wang<sup>1,3,4</sup>

<sup>1</sup>College of Integrated Chinese and Western Medicine, Hebei University of Chinese Medicine, Shijiazhuang, Hebei, 050091, People's Republic of China; <sup>2</sup>First Affiliated Hospital, Hebei University of Chinese Medicine, Shijiazhuang, Hebei, 050033, People's Republic of China; <sup>3</sup>College of Integrated Chinese and Western Medicine, Hebei University of Chinese Medicine, Hebei University of Chinese Medicine & Hebei Key Laboratory of Integrative Medicine on Liver-Kidney Patterns, Shijiazhuang, Hebei, 050091, People's Republic of China; <sup>4</sup>Second Affiliated Hospital, Hebei University of Chinese Medicine, Hebei, 073000, People's Republic of China

\*These authors contributed equally to this work

Correspondence: Yuehua Wang, Email wangyuehua@hebcm.edu.cn

**Purpose:** Preventing and treating diabetic nephropathy (DN) are global challenges due to the complexity and diversity of its causes and manifestations. It is important to find effective medications to treat DN.

**Patients and Methods:** Gene expression files of DN were downloaded from the GEO database to identify the differentially expressed genes. Network pharmacology and molecular docking were used to explore the possible mechanisms of modified Buyang Huanwu Decoction (mBHD) in treating DN. Biochemical, histopathological, and real-time PCR analyses were conducted in both in vivo and in vitro DN models to investigate the effects of mBHD.

**Results:** A total of 336 active ingredients and 124 potential targets of mBHD associated with DN were identified. Among them, 8 hub genes were found to be important targets for mBHD in treating DN and were significantly correlated with the infiltration status of six immune cells. Partially, the active ingredients of mBHD demonstrated good stability in binding to CASP3 and TP53. mBHD treatment significantly reduced levels of total cholesterol, triglyceride, blood urea nitrogen, serum creatinine, and microalbumin in db/db mice. HE and Masson's staining results showed that mBHD attenuated renal injury in db/db mice. Additionally, mBHD treatment could significantly alter the expression of CASP3, CCL2, TP53, ALB, and HMOX1.

**Conclusion:** mBHD may be involved in the treatment of DN through multiple ingredients, targets, and pathways. In addition, mBHD could alleviate renal injury in db/db mice, possibly involving CASP3, CCL2, TP53, ALB, and HMOX1.

**Keywords:** diabetic nephropathy, network pharmacology, molecular docking, traditional Chinese medicine

## Introduction

Diabetic nephropathy (DN) is a common microvascular complication of diabetes mellitus (DM) that leads to chronic kidney disease and end-stage renal disease.<sup>1</sup> Various factors, such as long-term hyperglycemia, extracellular matrix deposition, oxidative stress, and genetic factors, can contribute to the development of DN.<sup>2,3</sup> Current clinical treatments for DN are limited and mainly focus on controlling blood glucose, reducing blood pressure, and decreasing urinary protein.<sup>4,5</sup> However, the therapeutic effects of these methods are often suboptimal. Although some hypoglycemic agents, such as glucagon-like peptide 1 receptor agonists (GLP-1RAs) and sodium-dependent glucose transporters 2 inhibitors (SGLT2i), have been shown to offer renal protection, DM patients still face a high risk of developing kidney disease.<sup>6</sup>

Traditional Chinese medicine (TCM), with a history spanning thousands of years, has been widely utilized to improve quality of life and treat diseases.<sup>7</sup> Several studies have shown that TCM could be effective in treating DM

and its complications by mainly focusing on detoxification and reducing inflammation.<sup>8,9</sup> Modified Buyang Huanwu decoction (mBHD) is an improved formula derived from Buyang Huanwu Decoction (BHD) and Shenqi Dihuang Decoction (SDD). It was proposed based on Professor Zhao Yuyong's "renal collateral stasis" theory, supported by years of clinical experience. Individually, BHD and SDD have demonstrated good efficacy and safety in treating early-stage DN patients,<sup>10,11</sup> and mBHD combines the benefits of the two classical formulas. The main ingredients include 15 kinds of traditional herbs. Our previous studies have shown that mBHD inhibits renal tubulointerstitial fibrosis in db/db mice,<sup>12</sup> prevents high glucose-induced epithelial-mesenchymal transition of HK-2 cells,<sup>13</sup> and improves diabetic liver injury.<sup>14</sup> In addition, the combination of basic Western treatment with mBHD has been clinically effective in inhibiting the expression of inflammatory factors and ameliorating renal injury in patients with DN and has a favorable safety profile.<sup>15</sup> Therefore, mBHD is considered a promising therapeutic option for the treatment of DN. However, the mechanism of mBHD in DN remains unclear.

Network pharmacology has been utilized to study several TCM formulas in the treatment of diseases, aiming to elucidate the synergistic mechanism involving multiple ingredients, targets, and pathways.<sup>16,17</sup> In the present study, we comprehensively analyzed the pharmacological networks of mBHD in the treatment of DN using public data and identified hub genes, which were subsequently validated through *in vivo* and *in vitro* models.

## Materials and Methods

### Identification of Effective Ingredients, Target Genes, and Differentially Expressed Genes (DEGs)

A flowchart summarizing the study design is shown in [Figure 1](#). The Chinese medicine formulas of mBHD are listed in [Table 1](#). All of these herbs were in granule form, donated by Yifang Pharmaceutical Co. Ltd (Guangdong, China). The HERB database (<http://herb.ac.cn/>) was utilized to identify effective ingredients in 15 herbs and their corresponding target genes. The HERB database combines database mining and statistical inference to associate 7263 herbs and 49258 ingredients with 12933 targets and 28212 diseases, and provides six types of pairwise relationships.<sup>18</sup> GSE104948 (7 DN samples and 18 controls) and GSE96804 datasets (41 DN samples and 20 controls) acquired from the Gene Expression Omnibus (GEO) database were regarded as the training set and validation set, respectively. Differentially expressed analysis was performed on the GSE104948 dataset using the "limma" package (v3.36.5)<sup>19</sup> to identify DEGs associated with DN (FDR <0.05,  $|\log_2FC| > 0.2$ ).

### Enrichment Analysis

Target genes of 15 herbs and DEGs were intersected to obtain a Venn diagram of gene symbols (core genes). Database of Annotation, Visualization, and Integrated Discovery database (DAVID, <https://david.ncifcrf.gov/>) was employed to perform GO classification and KEGG pathway enrichment analysis for these core genes (FDR <0.05).<sup>20,21</sup> The screening results were visualized using the R package.

### Herb-Ingredient-Gene-Disease Network

We built a complex herb-ingredient-gene-disease network based on the interactions between 15 herbs, core genes, their corresponding active ingredients, and DN. Additionally, the network was visualized using Cytoscape v3.7.2 (<https://cytoscape.org/>).<sup>22</sup>

### Hub Genes Screening

Core genes were added into STRING (<https://string-db.org/>) and the results of protein-protein interaction (PPI) analysis were saved. CytoHubba, a plug-in of Cytoscape, was used to identify hub genes in the PPI network. Seven algorithms (MCC, MNC, EPC, Degree, Stress, Closeness and Betweenness) in cytoHubba were used to identify the hub genes in each algorithm.<sup>23</sup> Selecting the top 15 node genes based on the score from each algorithm, multicenter intersection genes were screened through the R package "UpSet" v1.4.0.<sup>24</sup>

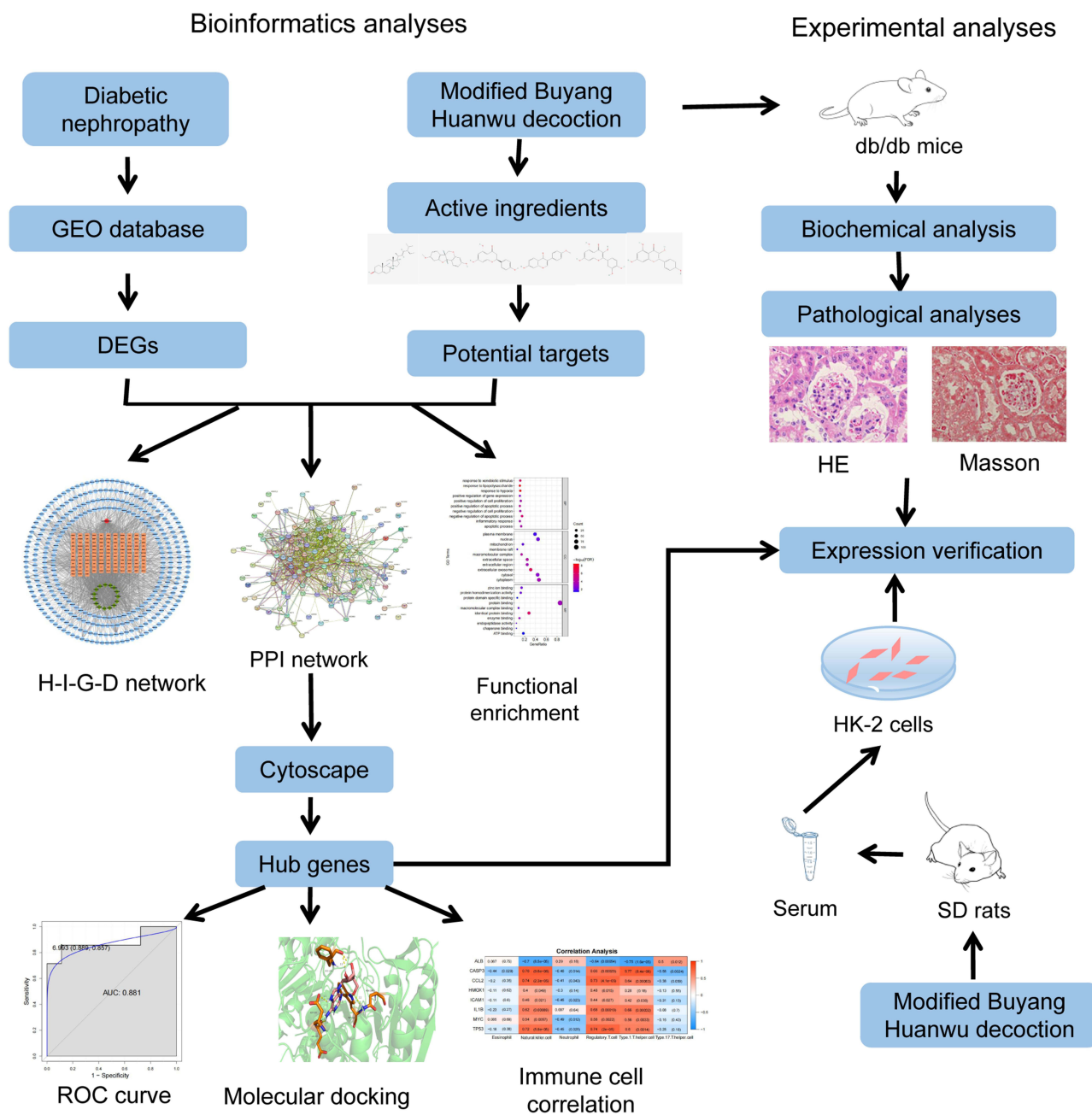


**Figure 1** A flowchart summarizing the study design. **Note:** Adapted from SciDraw (<https://scidraw.io/>). We gratefully acknowledge the contributions of Ethan Tyler, Lex Kravitz (DOI: 10.5281/zenodo.3925901), and Diogo Losch De Oliveira (DOI: 10.5281/zenodo.3926011) and DOI: 10.5281/zenodo.3925953) to SciDraw. **Abbreviations:** H-I-G-D network, herb-ingredient-gene-disease network; DEGs, differentially expression genes; ROC, receiver operating characteristic; PPI, protein-protein interaction.

## Immune Cell Infiltration Analysis

To measure the relative abundance of each cellular infiltrate in the immunological microenvironment (IME), the single-sample gene set enrichment analysis (ssGSEA) was applied. The gene set of infiltrated immune cells in IME was obtained from Charoentong’s study, which was enriched for a variety of human immune cell subtypes.<sup>25,26</sup> Wilcox test was used to compare the difference in immune cell infiltration between the DN and control groups. Additionally, the correlation analysis between hub genes and immune infiltrating cells was analyzed.

**Table 1** The Chinese Medicine Formulas of mBHD

Latin Name	Chinese Name	Lot Number	Granules
<i>Astragali Radix</i>	Huangqi	0093253	30 g
<i>Angelicae Sinensis Radix</i>	Danggui	0093103	10 g
<i>Paeoniae Radix Rubra</i>	Chishao	0113103	10 g
<i>Persicae Semen</i>	Taoren	0096363	10 g
<i>Pheretima</i>	Dilong	0106443	12 g
<i>Bombyx Batryticatus</i>	Jiangcan	0090403	10 g
<i>Cicadae Periostracum</i>	Chantui	9126463	6 g
<i>Pseudostellariae Radix</i>	Taizishen	0111323	15 g
<i>Atractylodis Macrocephalae Rhizoma</i>	Baishu	0113073	10 g
<i>Eupatorium japonicum Thunb</i>	Zelan	0092583	10 g
<i>Rehmanniae Radix Praeparata</i>	Shudihuang	0101963	15 g
<i>Dioscoreae Rhizoma</i>	Shanyao	0090453	15 g
<i>Moutan Cortex</i>	Mudanpi	0113783	10 g
<i>Poria</i>	Fuling	1307013	15 g
<i>Corni Fructus</i>	Shanzhuyu	0102693	10 g

## Receiver Operating Characteristic (ROC) Curve

The accuracy of hub genes in distinguishing DN patients from controls was evaluated using ROC curve analysis with the R package “pROC” (version 1.15.3).<sup>27</sup> The area under the curve (AUC) was calculated to assess the accuracy of the model. The expression of hub genes was validated in GSE96804 dataset and presented as box line plots.

## Molecular Docking

We performed molecular docking<sup>28</sup> to explore the binding activity of active ingredients and target genes and investigate the relationship between the two. The RCSB Protein Data Bank (PDB) database (<http://www.rcsb.org/pdb/home/home.do>) was used to retrieve the 3D structure files of target proteins (hub genes) as receptors,<sup>29</sup> while the 3D structure files of the active ingredients were downloaded from the PubChem (<https://pubchem.ncbi.nlm.nih.gov/>) database.<sup>30</sup> The protein receptors were pre-processed and removed water molecules using PyMOL,<sup>31</sup> followed by hydrogenation and other pretreatments using AutoDockTools.<sup>32</sup> A binding energy below 0 indicates spontaneous binding, with lower values signifying more stable ligand-receptor interactions. The docking results were visualized using PyMOL software.

## Experiment Animals and Medicine Intervention

Specific-pathogen-free (SPF) grade healthy male db/m (25±5 g) and db/db (45±5 g) mice, aged 11–12 weeks, were purchased from Changzhou Cavins Laboratory Animal Co., Ltd (Jiangsu, China). All mice were accommodated under controlled conditions including a 12-hour light/dark cycle, a temperature of 24±1°C, and a humidity range of 50%-70%. The mice were allowed to feed and drink freely throughout the study. A Certificate of Conformity: No. SCXK (Su) 2021–0013. The animal experiments were carried out under the permission of the animal ethics committee of our hospital (DWLL202203136) and in accordance with the ethical guidelines for animal experiments.

All mice were acclimatized to feeding for one week. The 16 db/db mice were monitored for all positive urine protein before being randomly divided into two groups (n = 8 per group): DM group and mBHD group, and the db/m group as the control (Con) group (n = 8). The mBHD group was administered and treated by mBHD (6.11 g/mL) with intra-gastric gavage once a day for 8 weeks (24.44 g/kg). The Con and DM groups were given an equal volume of distilled water daily. No other interventions were given during the experimental period, such as insulin or hypoglycemic agents. After medicine intervention, urine was obtained. After the mice were fasted for 12 h, they were anesthetized and executed, and the blood and kidneys were taken for subsequent experiments.

## Biochemical Analysis

Mice urine was centrifuged at 3000 r/min, 4°C for 5 min, and the supernatant was collected. The concentration of microalbumin (mALB) was measured by the mALB reagent kit according to the manufacturer's instructions. An automatic blood biochemistry analyzer was employed to detect biochemical indicators, including fasting blood glucose (FBG), total cholesterol (TC), triglyceride (TG), blood urea nitrogen (BUN), and serum creatinine (Scr).

## Histological Examination

The kidney tissues were fixed with 4% paraformaldehyde for 24 h. After paraffin-embedded sections, gradient dehydration, and xylene transparency, HE and Masson staining were performed, followed by observing the renal histopathological changes under the microscope. The pathology sections of Masson staining were analyzed using Image-Pro Plus 6.0 analysis software to calculate the collagen area (fibrosis).

## Cell Culture, Serum Preparation and Medicine Intervention

Human proximal tubular cells (HK-2 cells) were purchased from Cell Resource Center, Institute of Basic Medical Sciences, PUMC. HK-2 cells were grown at 37°C under 5% CO<sub>2</sub> and cultured using MEM medium containing 10% fetal bovine serum (FBS) and 1% P/S (Gibco, USA).

Thirty male SD rats of SPF grade, weighing 220–260 g, purchased from Viton Lihua Laboratory Animal Technology Co., Ltd (Beijing, China), were kept under the same conditions as above. Laboratory Animal License No. SCXK (Beijing) 2021–0011. Thirty rats were fed for 3 d and randomly divided into two groups (n = 15 per group): the blank serum group and mBHD serum group. The mBHD serum group were administered treated by mBHD with intra-gastric gavage twice a day for 7 d (24.44 g/kg/d), and the blank serum group was treated with an equal volume of drinking water. On day 7, the mBHD was administered twice with a 2-hour interval. One hour after the last administration, the blood was collected from the abdominal aorta after anesthesia with inhalation anesthesia (3% isoflurane). The serum was inactivated and sterilized for medical intervention.

Our previous study showed that the optimal administration concentrations were 10% and the optimal intervention time was 48 h.<sup>13</sup> Therefore, HK-2 cells were divided into three groups to perform medicine intervention for 48 h: low-glucose (LG) group (glucose 5.5 mmol/L + 10% blank serum), high-glucose (HG) group (glucose 30 mmol/L + 10% blank serum), and HG + mBHD group (glucose 30 mmol/L + 10% mBHD serum).

## Real-Time PCR

TRIzol reagent was used to extract total RNA from mouse kidney tissues and HK-2 cells, which was then reverted to cDNA using the RT First Strand cDNA Synthesis Kit (Servicebio, China). The expression levels of selected mRNAs were detected by real-time PCR. GAPDH was used as an internal reference gene. The reaction system was programmed as follows: incubation at 95°C for 10 min, followed by 40 cycles for 10s at 95°C, 15s at 58°C and 10s at 72°C. The 2<sup>-ΔΔCt</sup> method was used for estimating the gene expression levels and one-way ANOVA was performed using GraphPad Prism software (version 8, Boston, Massachusetts USA, [www.graphpad.com](http://www.graphpad.com)). The specific primer sequences are shown in [Table S1](#).

## Statistical Analysis

SPSS 25.0 software was used for statistical analysis, and the data were presented as mean±standard deviation, one-way ANOVA was used if the variance was unanimous, the SNK-q test was used for two-by-two comparisons, and the Kruskal–Wallis *H*-test was used if the variance was not unanimous, and *P* values <0.05 were considered statistically significant.

## Results

### Identification of Core Genes, Enrichment Analysis, and Network Construction

A total of 1636 active ingredients and 483 target genes were identified for 15 herbs using the HERB database. We identified 3345 DEGs in the DN group compared with controls based on the GSE104948 dataset, including 2305 up-

regulated genes and 1040 down-regulated genes (Figure S1A and B). These DEGs were overlapped with 483 target genes of herbs to obtain 124 intersecting genes (core genes) (Figure 2A), followed by GO and KEGG enrichment analysis. GO analysis showed that these core genes were mainly distributed in the cytoplasm, plasma membrane, and other cellular components. They were involved in molecular functions such as protein binding, ATP binding, zinc ion binding, and macromolecular complex binding, and participate in biological processes including cell proliferation and apoptosis, hypoxia, and inflammatory response (Figure 2B). The KEGG analysis indicated that these core genes were primarily enriched in the AGE-RAGE signaling pathway in diabetic complications, NF-κB, PI3K-Akt, and metabolic pathways (Figure 2C). Taken together, those results indicated that 15 herbs may play a therapeutic role in DN through its synergistic effects of multiple ingredients, pathways, and targets.

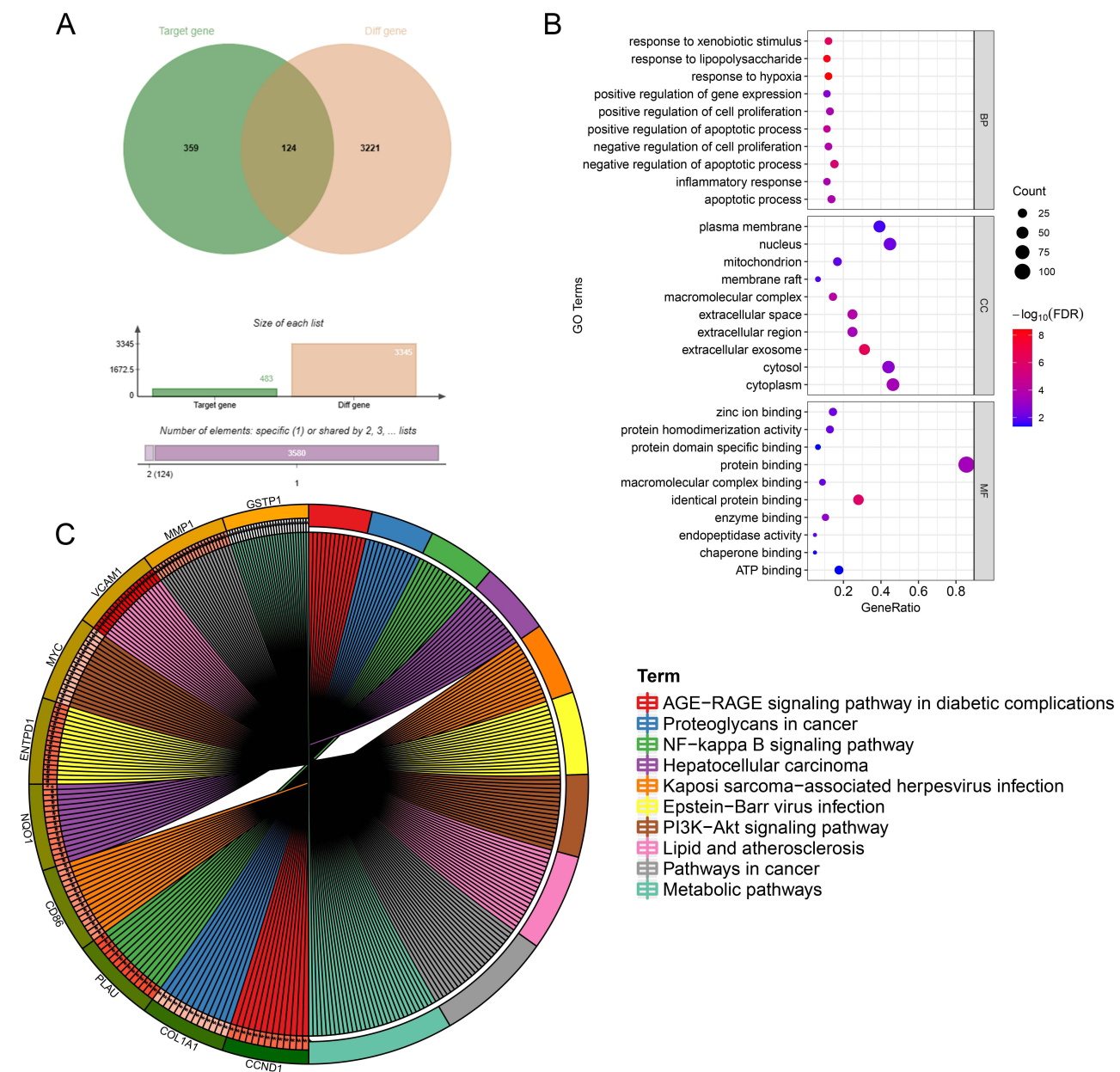


**Figure 2** Identification and functional enrichment analysis of core genes. **(A)** A Venn diagram shows that target genes of 15 herbs and DEGs overlapped to acquire 124 core genes (intersection). Circles indicate the collection of genes within different gene sets. **(B)** GO and **(C)** KEGG analysis of core genes.  $P < 0.05$  and false discovery rate (FDR)  $< 0.05$  were set as the cutoff criteria; the top 10 meaningful terms are presented in the bubble chart (GO) and cycle (KEGG).

# Construction of an Herb-Ingredient-Gene-Disease Network

An herb-ingredient-gene-disease network was established using the Cytoscape based on the interactions between 15 herbs, 124 core genes and their corresponding 336 active ingredients, and DN (Figure 3). Additionally, the top 15 core genes were identified based on the number of interactions with the ingredients, including PTGS1, ADRB2, CA2, CASP3, MAOA, AKR1B1, SLC6A4, BAX, ADRA2A, ADRB1, HMOX1, TP53, GATM, CASP8, and ICAM1 (Figure 4A).

## Identification of Hub Genes

The PPI network of 124 core genes, including 845 interactions, was constructed. The most genes interacting with TP53 in the network were 63 genes. With CytoHubba, 8 hub genes were identified, including ALB, TP53, IL1 $\beta$ , CASP3, MYC, CCL2, ICAM1, and HMOX1 (Figure 4B). The PPI network analysis of 8 hub genes was performed (Figure 4C). The

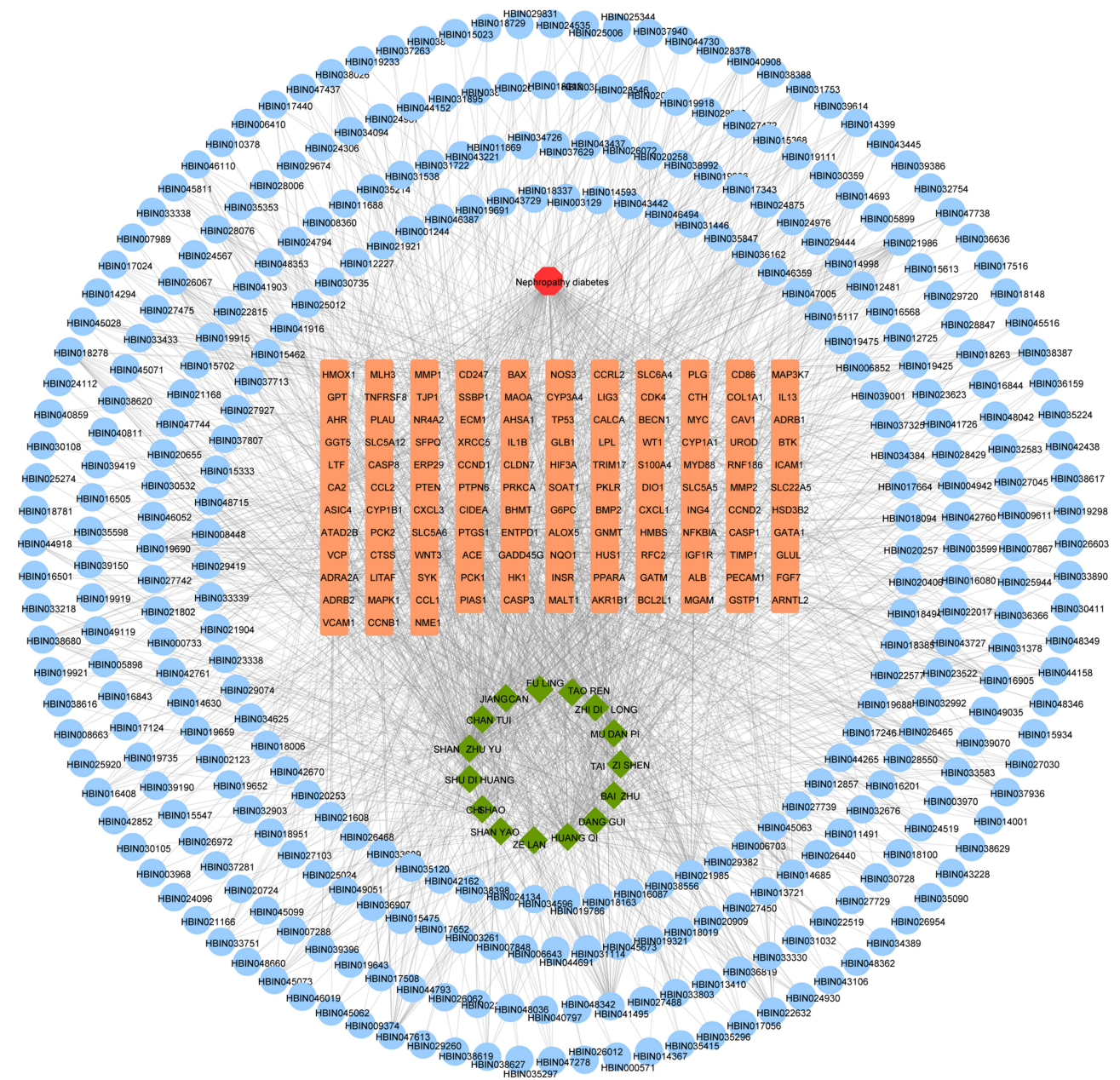


**Figure 3** Construction of an herb-ingredient-gene-disease network. A complex herb-ingredient-gene-disease network was constructed by STRING and Cytoscape based on the interactions between 15 herbs (green), 336 active ingredients (blue), 124 core genes (Orange), and DN (red).

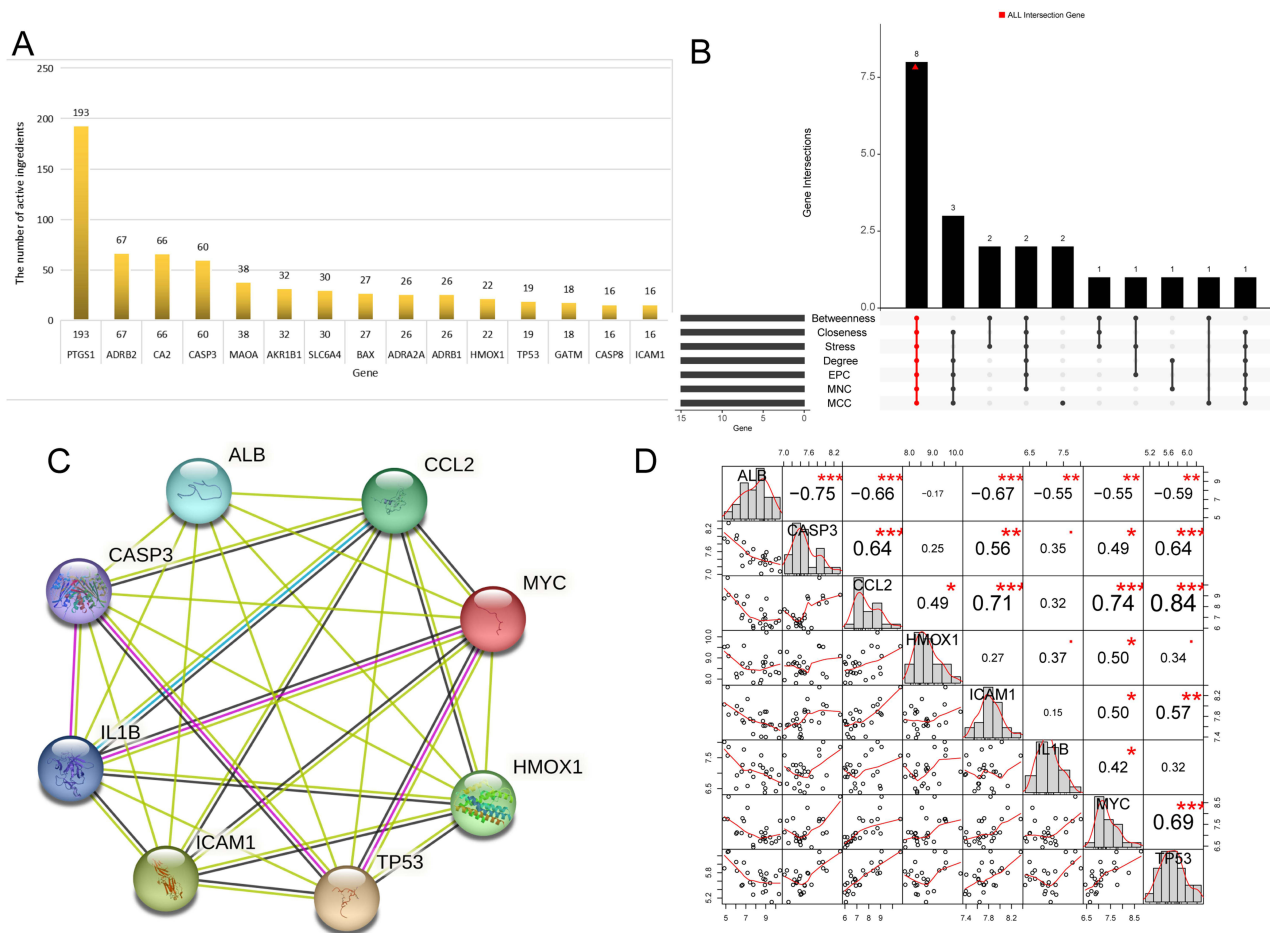


**Figure 4** Identification of hub genes. (A) The top 15 core genes were identified based on the number of interactions with the ingredients. (B) Identification of hub genes using seven algorithms within CytoHubba. The top 15 genes were selected based on their scores from each algorithm, and the multicenter intersection genes were identified as hub genes. (C) The PPI network of hub genes. Different colored lines represent evidence of interactions from different sources (D) The Pearson correlation analysis of hub genes. A larger font size indicates a stronger correlation.

results showed that a total of 28 interactions were identified, in which 3 had a score of at least 0.9, including CCL2 and IL1β (0.993), CASP3 and TP53 (0.925), and MYC and TP53 (0.923). Meanwhile, each of hub genes interacted with other genes. The correlation analysis of 8 hub genes suggested that TP53 and CCL2 had the strongest positive correlation ( $r = 0.84$ ), and CASP3 and ALB had the strongest negative correlation ( $r = -0.75$ ). Meanwhile, only the MYC gene had a significant correlation with all the other hub genes (Figure 4D).

### Immune Cell Infiltration Analysis

The infiltration status of 23 immune cells in the datasets of GSE104948 and GSE96804 was evaluated using ssGSEA analysis (Figure 5A and B). The results indicated that the infiltration levels of natural killer cells, regulatory T cells, and type 1 T helper cells 4 were significantly higher in the DN group compared to the control group in both two datasets. On the other hand, the infiltration levels of Eosinophil, Neutrophil, and Type 17 T helper cells were lower in the DN group. In addition, the correlation analysis of these 6 immune cells and 8 hub genes showed that CASP3 and Type 1 T helper cells had the strongest correlation ( $r = 0.77$ ), and CASP3 was significantly correlated with all 6 immune cells. Furthermore, Natural killer cells and Type 1 T helper cells were significantly correlated with all hub genes (Figure 5C).

### ROC Curve Analysis of Hub Genes

The ROC curve analysis showed that ALB, TP53, IL1β, CASP3, and CCL2 all had a diagnostic AUC of more than 0.7, indicating good sensitivity and specificity of those genes (Figure 6 and S2A). The expression levels of 8 hub genes in the



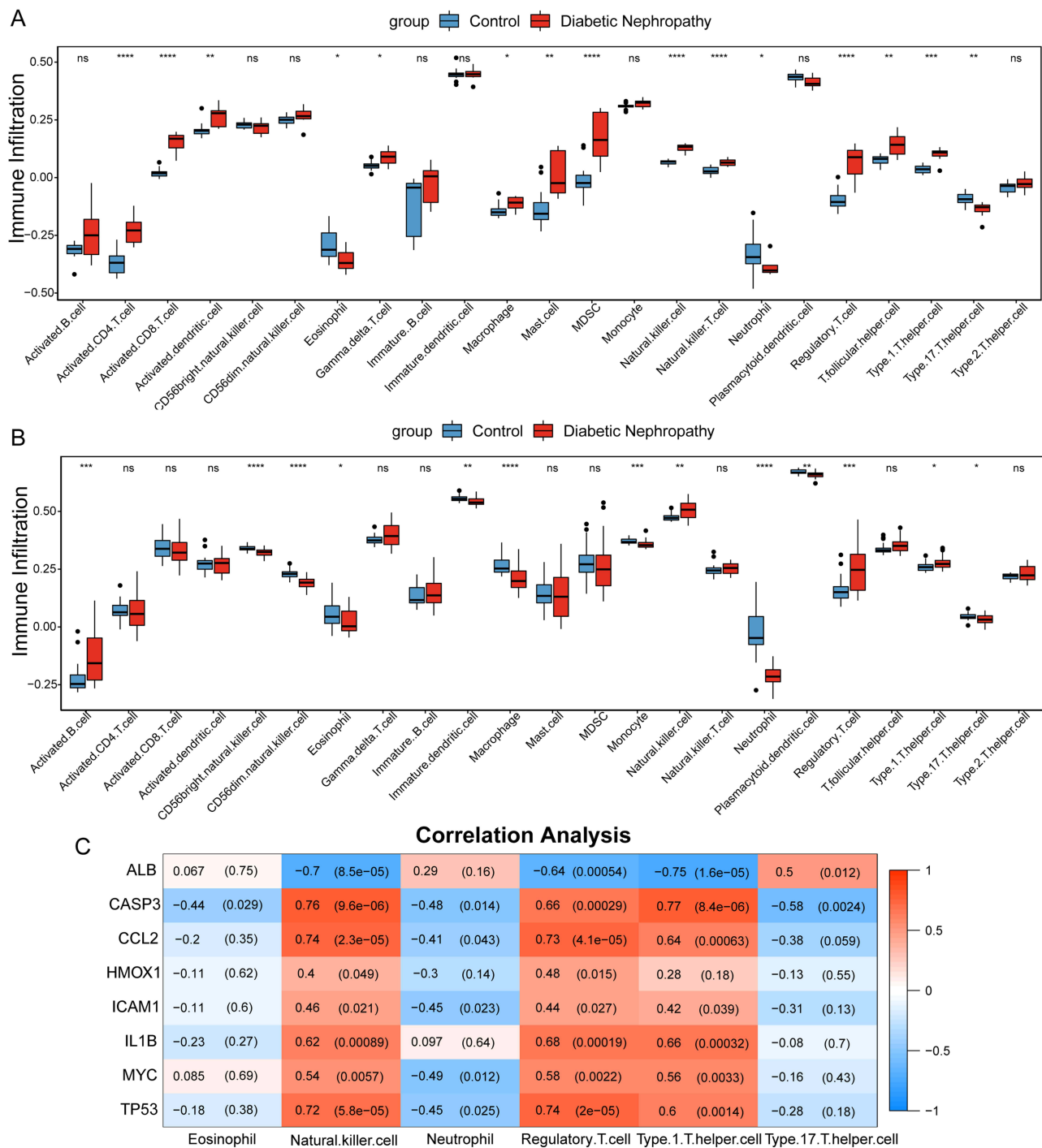


**Figure 5** Immune cell infiltration and hub genes. **(A)** Immune cell infiltration analysis evaluated the abundance of 23 immune cells in control and DN groups using ssGSEA in the GSE104948 dataset. **(B)** Immune cell infiltration analysis in the GSE96804 dataset. **(C)** The correlation analysis between identified immune cells and hub genes. Red represents positive correlations and blue represents negative correlations. The numbers in the boxes represent correlation coefficients (left) and *p*-values (right). \**P* < 0.05, \*\**P* < 0.01, \*\*\**P* < 0.001, \*\*\*\**P* < 0.0001.

GSE104948 dataset were presented in Table 2. In addition, we also verified the expression of hub genes in the GSE96804 dataset and found that the expression levels of ALB, TP53, CASP3, ICAM1, MYC, and CCL2 were significantly different in the DN group compared to the control group (Figure S2B).

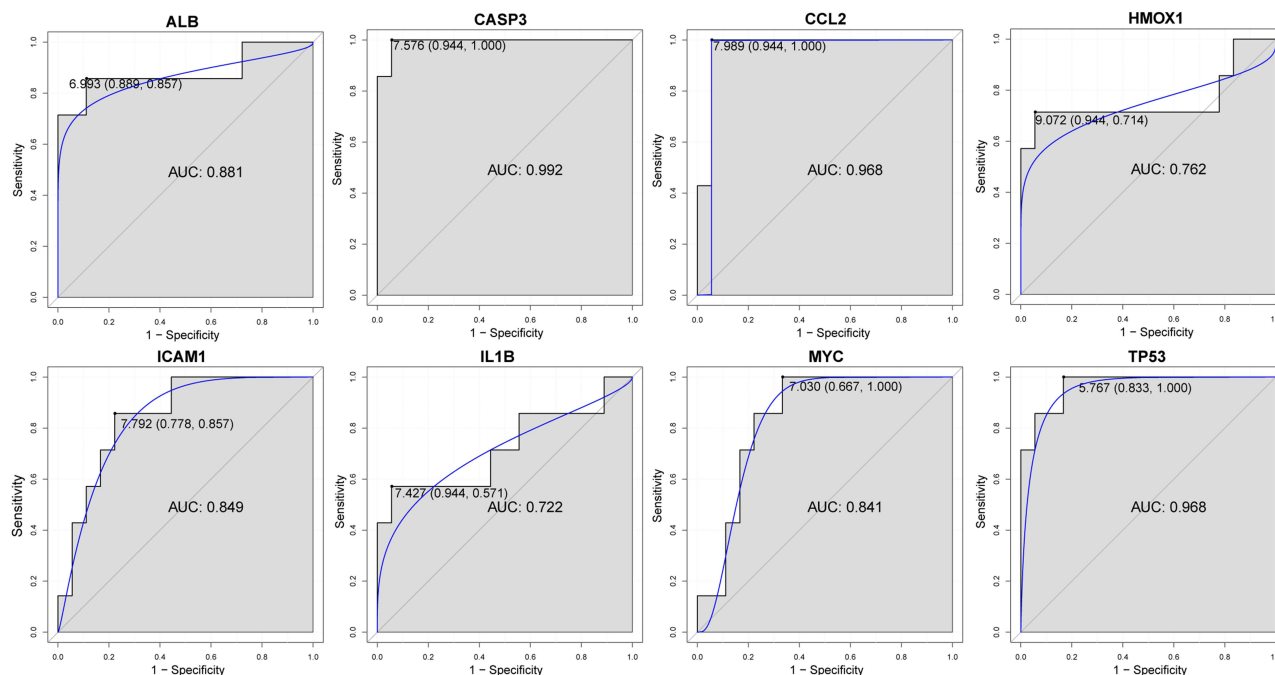


**Figure 6** ROC curve analysis of hub genes in the GSE104948 dataset. ROC curve analysis of 8 hub genes. A specific threshold point is marked on the curve with the corresponding sensitivity and specificity.

## Molecular Docking

Based on the above results, we finally selected CASP3 and TP53 for molecular docking. The top 10 active ingredients were identified based on the number of interactions with the 124 core genes (Table 3). Subsequently, CASP3 and TP53 were analyzed and docked with the top 10 active ingredients, respectively (Figure 7). Among these, curcumin and curcumine have the same three-dimensional structure while no related three-dimensional structure was found for dandelion game ethyl alcohol. Typically, a binding energy of less than  $-5.0$  kJ/mol signifies good binding activity for both molecules.<sup>33</sup> The results showed that CASP3 and TP53 exhibited a stabilizing binding capacity with curcumin ( $-6.10/-6.13$  kJ/mol), quercetin ( $-5.51/-6.63$  kJ/mol), and ursolic acid ( $-9.19/-8.25$  kJ/mol).

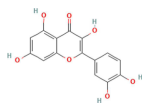
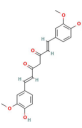
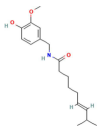
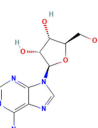
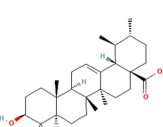
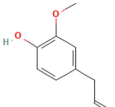
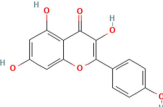
## mBHD Treatment Alleviates Renal Injury in Db/Db Mice

The levels of FBG, TG, and TC were significantly increased in the DM group compared with the control group. The levels of TG and TC were significantly decreased in the mBHD group compared with the DM group, while the levels of FBG were not significantly different between the two groups (Figure 8A). Furthermore, the levels of BUN, Scr, and mALB were significantly increased in the DM group compared with the control group. These results were reversed in the mBHD group (Figure 8A).

**Table 2** The Expression Levels of the Hub Genes in GSE104948

Gene name	log <sub>2</sub> FoldChange	p-value	Adj_p-value	Regulation
ALB	-2.388027485	8.81E-05	0.001041522	down
CASP3	0.583122902	2.50E-07	1.33E-05	up
CCL2	2.175008192	2.62E-07	1.37E-05	up
HMOX1	0.70026413	0.003762299	0.017297493	up
ICAM1	0.281217277	0.004661775	0.020142076	up
IL-1β	0.456057808	0.013742326	0.044812639	up
MYC	0.62257652	0.006021115	0.024366769	up
TP53	0.487649843	1.74E-05	0.000308755	up

**Table 3** The Top 10 Active Ingredients Were Identified Based on the Number of Interactions with the 124 Core Genes

Ingredient ID	Ingredient Name	Structure	Source	Interacting Number	Interacting Hub Genes
HBIN041495	quercetin		Mudanpi, Huangqi, Shanzhuyu	38	CASP3, HMOX1, TP53, CCL2, IL1 $\beta$ , MYC, ICAMI
HBIN021985 (HBIN021986)	curcumin (curcumine)		Danggui, Shanzhuyu (Shanzhuyu)	34 (32)	CASP3, TP53, CCL2, IL1 $\beta$ , MYC, HMOX1, ICAMI
HBIN019690	capsaicin		Huangqi	25	CASP3, TP53, HMOX1, MYC, ALB
HBIN014685	adeninenucleoside		Huangqi, Shanyao, Danggui	22	HMOX1, CASP3, TP53, MYC
HBIN022632	Dandelion game ethyl alcohol	Not Found	Taizhishen	21	CASP3, TP53, ICAMI
HBIN047613	ursolic acid		Taizhishen, Zelan, Shanzhuyu	20	CASP3, TP53, ICAMI, CCL2, IL1 $\beta$
HBIN026067	eugenol		Shanzhuyu, Chishao, Mudanpi, Shanyao	19	HMOX1, CASP3, CCL2, IL1 $\beta$
HBIN031753	kaempferol		Mudanpi, Huangqi, Taizhishen, Chishao	17	CASP3, HMOX1, ICAMI
HBIN016905	arsenic	Not Found	Chantui	16	None

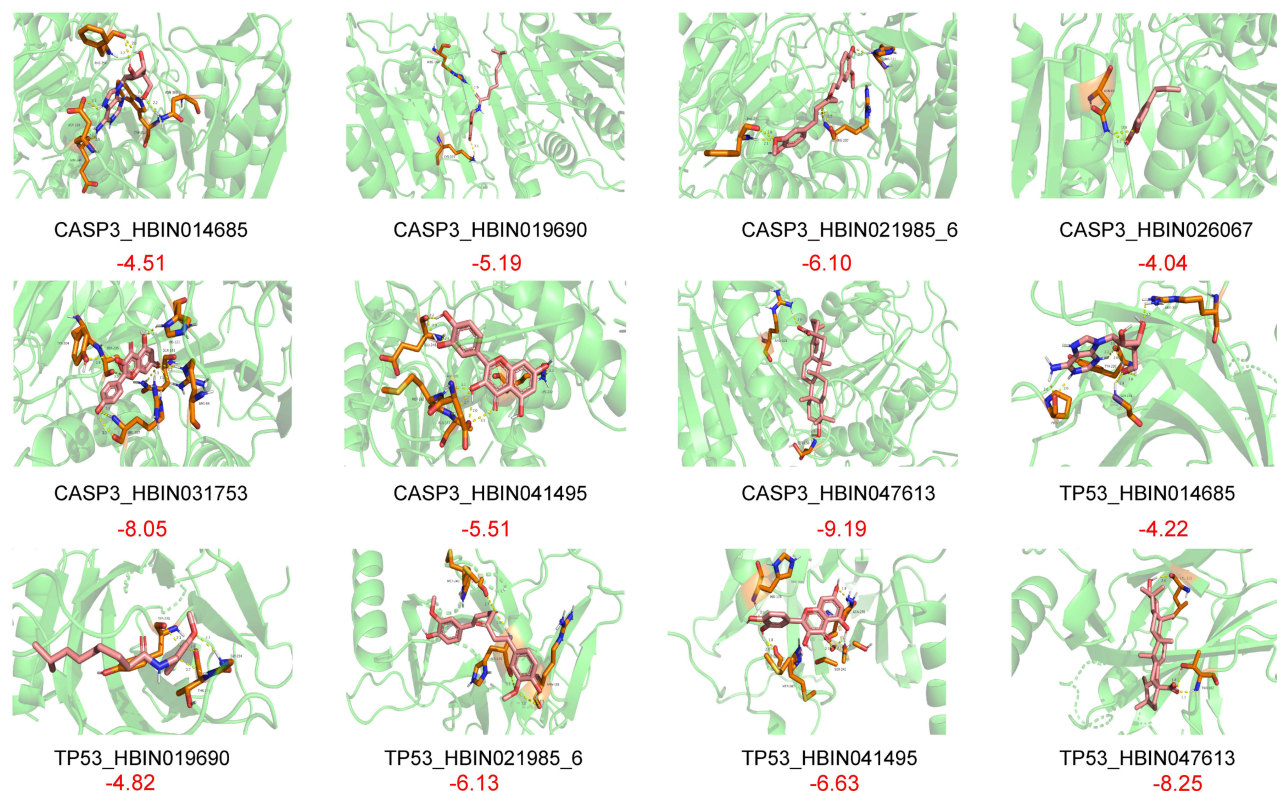


**Figure 7** The molecular docking of hub genes and active ingredients. The red font represents the minimum binding energy (kJ/mol). The protein structure is depicted in green ribbons. Key residues involved in the interaction are shown in Orange sticks. The docked ingredients are displayed in pink sticks. Hydrogen bonds between the ingredient and the protein residues are indicated by yellow dashed lines, with distances labeled in angstroms (Å).

In addition, HE and Masson were used to explore the effects of mBHD on renal histopathology in DM mice (Figure 8B). The renal tissue structure of mice in the control group was clear. Compared with the control group, the glomeruli of mice in the DM group were hypertrophied, the extra-membranous matrix increased, the basement membrane thickened, the cystic lumen narrowed, the interstitial inflammatory cells infiltrated, and partially the interstitial fibrosis. This renal injury was significantly ameliorated in the mBHD group. Taken together, mBHD could alleviate pathology and renal injury in db/db mice.

## Verification of Hub Gene Expression in Both in vivo and in vitro DN Models

We detected the expression levels of hub genes in kidney tissues of mice models with DN. The mRNA levels of CASP3, CCL2, IL-1 $\beta$ , and TP53 were significantly increased in the DM group compared with controls, while the mRNA levels of ALB and HMOX1 were significantly decreased, and the levels of ICAM1 and MYC were not significantly different between the two groups. The mRNA levels of CASP3, CCL2, IL-1 $\beta$ , TP53, ALB, and HMOX1 were reversed in the mBHD group (Figure 9A). The results in the high glucose-induced HK-2 cell injury model were consistent with these findings, except for IL-1 $\beta$ , which did not change significantly after mBHD treatment (Figure 9B).

## Discussion

DN is a severe complication of DM, with a mortality rate approximately 30 times higher than that of DM patients without kidney disease.<sup>34</sup> Preventing and treating DN is a global challenge due to its intricate causes and manifestations.<sup>3,34</sup> TCMs have been shown to improve kidney function and can be effective in the treatment of DN.<sup>9</sup> Using network pharmacology, molecular docking, and experimental methods, we explored the therapeutic potential of mBHD in DN, aiming to identify potential therapeutic targets and provide more precise treatment guidance.

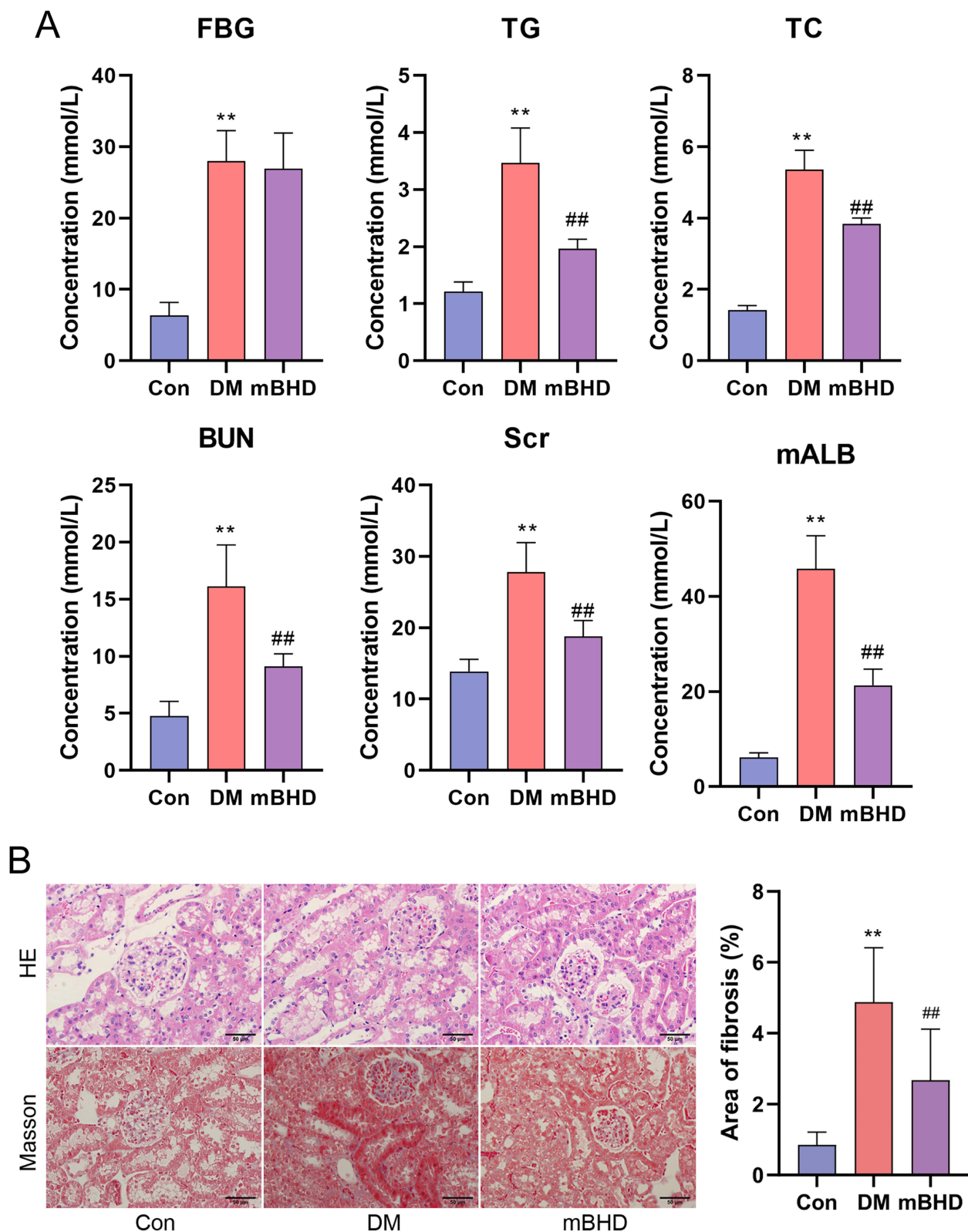


**Figure 8** Amelioration of DN in db/db mice treated with mBHD. **(A)** The levels of FBG, TG, TC, BUN, Scr, and mALB. N = 8. **(B)** HE and Masson staining (left) (original magnification $\times 400$ , scale bar = 50  $\mu\text{m}$ ). The percentage of fibrosis area was evaluated using Masson staining in pathology sections (right, n = 6). \*\* $P < 0.01$  vs Con group. ### $P < 0.01$  vs DM group.

**Abbreviations:** FBG, fasting blood glucose. TG, triglyceride. TC, total cholesterol. BUN, blood urea nitrogen. Scr, serum creatinine. mALB, microalbumin. Con, control. DM, diabetes mellitus. mBHD, modified Buyang Huanwu Decoction.

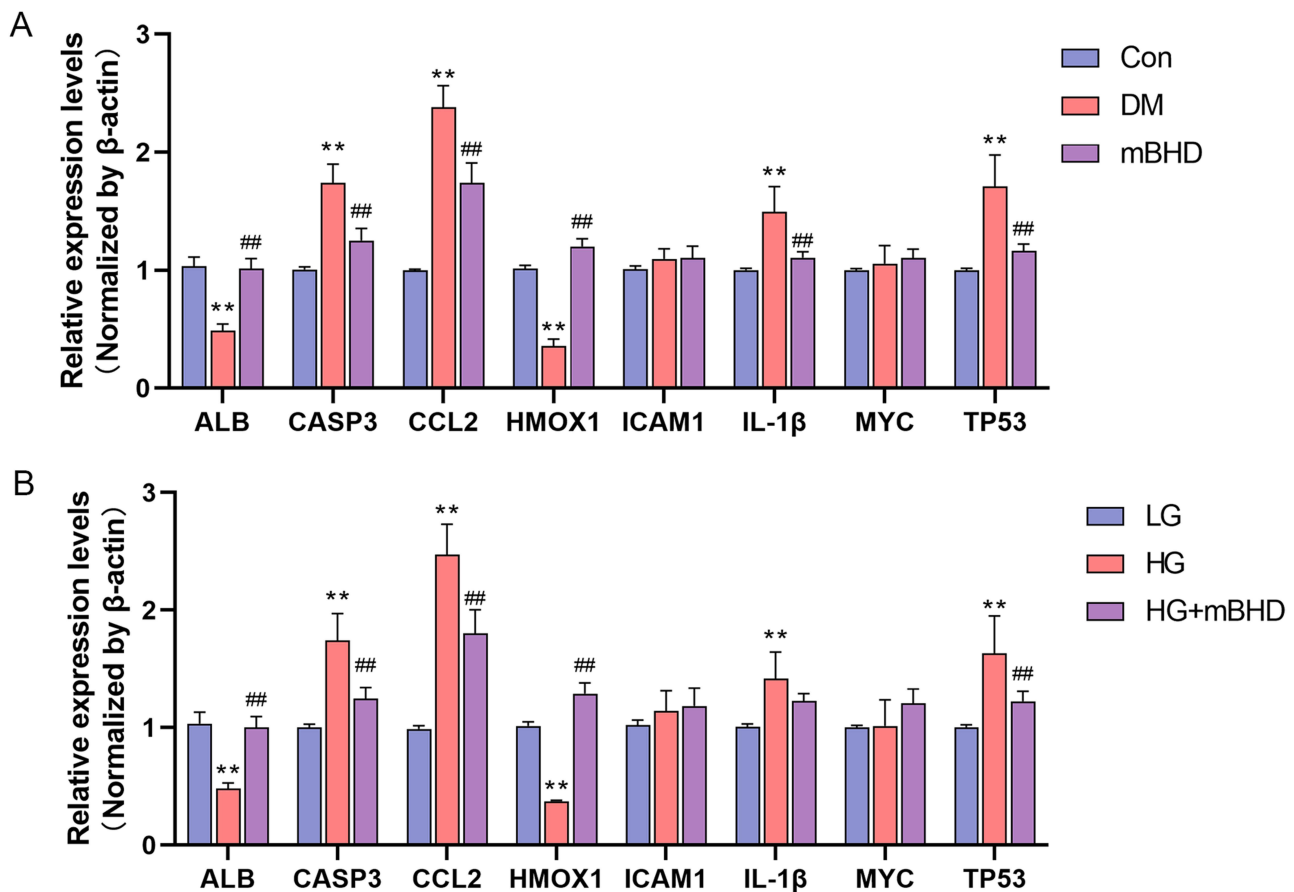


**Figure 9** Expression levels of hub gene in DN models. The mRNA levels of ALB, TP53, IL1β, CASP3, MYC, CCL2, ICAM1, and HMOX1 were detected using real-time PCR. (A) In db/db mice model (B) In High glucose-induced HK-2 cells model. \*\**P* <0.01 vs Con group. ##*P* <0.01 vs DM group. N = 3.

The GO analysis of 124 core genes revealed that these potential targets may be involved in cell proliferation/apoptosis, and response to reactive oxygen species and inflammation. These pathways were closely related to DN pathogenesis,<sup>35</sup> suggesting a crucial role for mBHD in DN treatment. KEGG analysis indicated that active ingredients in mBHD may affect DN through the AGE-RAGE, NF-κB, PI3K/AKT signaling pathway, and metabolic pathways. Advanced glycation end products (AGEs), markers of DN, bind to their specific receptor, RAGE, mediating oxidative stress and chronic inflammation, which lead to kidney injury.<sup>36</sup> The AGE-RAGE signaling pathway could promote the expression of NF-κB.<sup>37</sup> Inhibition of PI3K/AKT has been associated with reduced inflammation in DN mice.<sup>38</sup> Metabolic disorders are strongly associated with the progression of DN.<sup>34</sup> Therefore, we hypothesized that mBHD alleviates DN mainly through these pathways involving advanced glycosylation products, oxidative stress, inflammatory response, apoptosis, and metabolism.

Further analysis using Cytoscape identified eight hub genes: ALB, TP53, IL1β, CASP3, MYC, CCL2, ICAM1, and HMOX1. ROC curve analysis demonstrated their specificity and sensitivity in diagnosing DN. Notably, the expressions of CASP3, CCL2, TP53, ALB, and HMOX1 exhibit significant differences after mBHD treatment in both mouse and cell models. Podocyte apoptosis is a typical early feature of DN, and CASP3 and TP53 are involved in DN progression by regulating podocyte apoptosis.<sup>39,40</sup> CCL2 blockade improves macrophage infiltration and oxidative stress in DN mice.<sup>41</sup> HMOX1 may play a role in developing renal microangiopathy in DN.<sup>42</sup> ALB encodes albumin, the most abundant protein in human blood, which is significantly reduced in patients with DN and associated with DN prognosis.<sup>43</sup> Therefore, CASP3, CCL2, TP53, ALB, and HMOX1 may be key targets of mBHD for DN treatment.

Immune and inflammatory responses are key courses of DN, and the degree of immune cell infiltration is directly related to the severity of DN.<sup>44</sup> Immune cell infiltration analysis in this study found that six types of immune cells exhibited significant differences between DN patients and controls. The progression of DN may involve these six types of

immune cells. Notably, natural killer cells and type 1 T helper cells showed correlations with hub genes. Dysfunction of natural killer cells is observed in end-stage renal disease.<sup>45</sup> The balance between type 1 and type 2 T-helper cells could regulate inflammatory pathways and macrophage infiltration, influencing the progression of DN.<sup>46</sup> Thus, the treatment of DN by mBHD may partly manifest in modulating the immune cell infiltration process.

The significant differential expression of CASP3 and TP53 between DN and control samples, combined with their good diagnostic ability for DN, interaction with multiple active ingredients and targets, and a significant correlation between CASP3 and immune infiltrating cells, made them promising candidates for further study. Molecular docking of these two genes with the top 10 active ingredients revealed stable binding of CASP3 and TP53 to curcumin, quercetin, and ursolic acid, ingredients known to be implicated in various DN pathways, including oxidative stress, inflammation, fibrosis, apoptosis, and autophagy.<sup>47–49</sup> Moreover, herbs-ingredients-targets-DN correspondences revealed that herbs Shanzhuyu, Huangqi, and Taizhishen in mBHD may target CASP3 and TP53 through these three active ingredients. Studies have shown that curcumin and quercetin can inhibit podocyte apoptosis in DN by regulating the expression of CASP3.<sup>50,51</sup> These findings underscore the complexity and versatility of mBHD's therapeutic approach in DN, engaging multiple active ingredients and targeting a diverse array of key genes.

Biochemical and histopathological analyses indicated that mBHD could significantly ameliorate renal injury in db/db mice. Moreover, consistent with the results of BHD treatment in DN mice,<sup>52</sup> mBHD reduced the levels of mALB in db/db mice without affecting their FBG levels, suggesting that the therapeutic effect of mBHD on DN may be directly through the protection of renal function. Therefore, mBHD could be a new promising therapeutic strategy for DN.

The accuracy of results in network pharmacology is constrained by algorithm selection, with different algorithms potentially yielding varying outcomes.<sup>53</sup> Network pharmacology cannot quantify the dose-efficacy relationship between drugs and diseases. Current research is further limited by bioinformatics analyses, and the potential targets and pathways of mBHD's action on DN need validation through extensive *in vivo* and *in vitro* studies. While mBHD has shown preliminary efficacy in DN, it is crucial to assess its toxicity thoroughly.<sup>54</sup>

## Conclusion

In conclusion, mBHD may be involved in the treatment of DN through AGE-RAGE, NF- $\kappa$ B, PI3K/AKT, and metabolic pathways. In addition, mBHD treatment could significantly alter the expression of CASP3, CCL2, TP53, ALB, and HMOX1 and ameliorate renal injury. These findings offer valuable insights for the clinical application of mBHD. Future research should focus on conducting experimental models to confirm these findings. Additionally, exploring the long-term effects and potential interactions with other therapeutic agents would provide a more comprehensive understanding of its clinical applicability.

## Data Sharing Statement

The datasets used and/or analysed during the current study are available from the corresponding author on reasonable request.

## Ethics Approval and Informed Consent

This study was approved by the Ethics Committee of Hebei University of Chinese Medicine (DWLL202203117). All protocols on mice were carried out according to the National Institutes of Health Guidelines for the Care and Use of Laboratory Animals. All methods were conducted in accordance with the ARRIVE guidelines (<https://arriveguidelines.org>).

## Author Contributions

All authors made a significant contribution to the work reported, whether that is in the conception, study design, execution, acquisition of data, analysis and interpretation, or in all these areas; took part in drafting, revising or critically reviewing the article; gave final approval of the version to be published; have agreed on the journal to which the article has been submitted; and agree to be accountable for all aspects of the work.

## Funding

This study was supported by the Natural Science Foundation of Hebei Province of China (H2022423320, H2022423342), Key project of Hebei Province Education Department (ZD2021081), Project of Hebei Province Key R&D Program (223777150D) and the Natural Science Foundation of China (82274504).

## Disclosure

The authors report no conflicts of interest in this work.

## References

- Kim SS, Kim JH, Kim JJ. Current challenges in diabetic nephropathy: early diagnosis and ways to improve outcomes. *Endocrinol Metab.* 2016;31(2):245–253. doi:10.3803/EnM.2016.31.2.245
- Bhattacharjee N, Barma S, Konwar N, Dewanjee S, Manna P. Mechanistic insight of diabetic nephropathy and its pharmacotherapeutic targets: an update. *Eur J Pharmacol.* 2016;791:8–24. doi:10.1016/j.ejphar.2016.08.022
- Samsu N. Diabetic Nephropathy: challenges in Pathogenesis, Diagnosis, and Treatment. *Biomed Res Int.* 2021;2021:1497449. doi:10.1155/2021/1497449
- Hu Q, Chen Y, Deng X, et al. Diabetic nephropathy: focusing on pathological signals, clinical treatment, and dietary regulation. *Biomed Pharmacother.* 2023;159:114252. doi:10.1016/j.biopha.2023.114252
- Tziomalos K, Athyros VG. Diabetic Nephropathy: new Risk Factors and Improvements in Diagnosis. *Rev Diabetic Stud.* 2015;12(1–2):110–118. doi:10.1900/RDS.2015.12.110
- Tuttle KR. The landscape of diabetic kidney disease transformed. *Nat Rev Nephrol.* 2020;16(2):67–68. doi:10.1038/s41581-019-0240-6
- Wang S, Long S, Deng Z, Wu W. Positive Role of Chinese Herbal Medicine in Cancer Immune Regulation. *Am J Chin Med.* 2020;48(7):1577–1592. doi:10.1142/S0192415X20500780
- Zhang TT, Jiang JG. Active ingredients of traditional Chinese medicine in the treatment of diabetes and diabetic complications. *Expert Opin Invest Drugs.* 2012;21(11):1625–1642. doi:10.1517/13543784.2012.713937
- Liu XJ, Hu XK, Yang H, et al. A Review of Traditional Chinese Medicine on Treatment of Diabetic Nephropathy and the Involved Mechanisms. *Am J Chin Med.* 2022;50(7):1739–1779. doi:10.1142/S0192415X22500744
- Zhao J, Mo C, Meng LF, Liang CQ, Cao X, Shi W. [Efficacy and safety of Buyang Huanwu Decoction for early-stage diabetic nephropathy: a Meta-analysis]. *Zhongguo Zhong yao za zhi.* 2019;44(8):1660–1667. Polish. doi:10.19540/j.cnki.cjmm.20190109.001
- Wang MR, Yu LH, Wang TT, Wang YM, Han MX. [Effect of Shenqi Dihuang decoction on inflammatory factor, renal function and microcirculation in patients with early diabetic nephropathy]. *Zhongguo Zhong yao za zhi.* 2018;43(6):1276–1281. Polish. doi:10.19540/j.cnki.cjmm.2018.0050
- Shuai Guo LB, Pan L, Guo L, Wang Y. Effect and mechanism of revised Buyang Huanwu Decoction combining with Shenqi Dihuang Decoction on renal tubulointerstitial fibrosis in diabetic nephropathy mice. *Zhong Cao Yao.* 2022;52(2):470–477. doi:10.7501/j.issn.0253-2670.2022.02.017
- Shuai Guo JF, Guo L, Wang Y, Pan L. Effect and mechanism study on high glucose-induced mesenchymal transformation of human renal tubular epithelial cell lines in treatment of serum containing Buyang Huanwu Decoction combined with Shenqi Dihuang Decoction. *China J Basic Chin Med.* 2022;28(8):1290–1295. doi:10.19945/j.cnki.issn.1006-3250.20211012.001
- Zhang X, Yang F, Zhang Y, et al. Modified Buyang Huanwu Decoction alleviates diabetic liver injury via inhibiting oxidative stress in db/db mice. *Am J Transl Res.* 2024;16(1):39–50. doi:10.62347/OYAQ7465
- Yuehua Wang FY, Yun M, shuai G, Lifei L, Jiaan H, Zhiqiang C. Clinical efficacy of Buyang Huanwu Decoction combined with Shenqi Dihuang Decoction in treatment of III-IV stage diabetic kidney disease and its protective effect on renal tubular injury. *Chin Traditional Herbal Drugs.* 2023;54(16):5289–5295. doi:10.7501/j.issn.0253-2670.2023.16.018
- Zheng W, Qian C, Xu F, et al. Fuxin Granules ameliorate diabetic nephropathy in db/db mice through TGF- $\beta$ 1/Smad and VEGF/VEGFR2 signaling pathways. *Biomed Pharmacother.* 2021;141:111806. doi:10.1016/j.biopha.2021.111806
- Le DH, Le L. Systems Pharmacology: a Unified Framework for Prediction of Drug-Target Interactions. *Curr Pharm Des.* 2016;22(23):3569–3575. doi:10.2174/1381612822666160418121534
- Fang S, Dong L, Liu L, et al. HERB: a high-throughput experiment- and reference-guided database of traditional Chinese medicine. *Nucleic Acids Res.* 2021;49(D1):D1197–d1206. doi:10.1093/nar/gkaa1063
- Ritchie ME, Phipson B, Wu D, et al. limma powers differential expression analyses for RNA-sequencing and microarray studies. *Nucleic Acids Res.* 2015;43(7):e47. doi:10.1093/nar/gkv007
- Sherman BT, Hao M, Qiu J, et al. DAVID: a web server for functional enrichment analysis and functional annotation of gene lists (2021 update). *Nucleic Acids Res.* 2022;50(W1):W216–w221. doi:10.1093/nar/gkac194
- Huang da W, Sherman BT, Lempicki RA. Systematic and integrative analysis of large gene lists using DAVID bioinformatics resources. *Nat Proto.* 2009;4(1):44–57. doi:10.1038/nprot.2008.211
- Shannon P, Markiel A, Ozier O, et al. Cytoscape: a software environment for integrated models of biomolecular interaction networks. *Genome Res.* 2003;13(11):2498–2504. doi:10.1101/gr.1239303
- Chin CH, Chen SH, Wu HH, Ho CW, Ko MT, Lin CY. cytoHubba: identifying hub objects and sub-networks from complex interactome. *BMC Syst Biol.* 2014;8(Suppl 4):S11. doi:10.1186/1752-0509-8-S4-S11
- Conway JR, Lex A, Gehlenborg N. UpSetR: an R package for the visualization of intersecting sets and their properties. *Bioinformatics.* 2017;33(18):2938–2940. doi:10.1093/bioinformatics/btx364
- Charoentong P, Finotello F, Angelova M, et al. Pan-cancer Immunogenomic Analyses Reveal Genotype-Immunophenotype Relationships and Predictors of Response to Checkpoint Blockade. *Cell Rep.* 2017;18(1):248–262. doi:10.1016/j.celrep.2016.12.019
- Barbie DA, Tamayo P, Boehm JS, et al. Systematic RNA interference reveals that oncogenic KRAS-driven cancers require TBK1. *Nature.* 2009;462(7269):108–112. doi:10.1038/nature08460
- Robin X, Turck N, Hainard A, et al. pROC: an open-source package for R and S+ to analyze and compare ROC curves. *BMC Bioinf.* 2011;12:77. doi:10.1186/1471-2105-12-77
- Kitchen DB, Decornez H, Furr JR, Bajorath J. Docking and scoring in virtual screening for drug discovery: methods and applications. *Nat Rev Drug Discov.* 2004;3(11):935–949. doi:10.1038/nrd1549
- Burley SK, Berman HM, Kleywegt GJ, Markley JL, Nakamura H, Velankar S. Protein Data Bank (PDB): the Single Global Macromolecular Structure Archive. *Methods Mol Biol.* 2017;1607:627–641. doi:10.1007/978-1-4939-7000-1\_26
- Kim S, Chen J, Cheng T, et al. PubChem 2023 update. *Nucleic Acids Res.* 2023;51(D1):D1373–d1380. doi:10.1093/nar/gkac956



31. Baugh EH, Lyskov S, Weitzner BD, Gray JJ. Real-time PyMOL visualization for Rosetta and PyRosetta. *PLoS One*. 2011;6(8):e21931. doi:10.1371/journal.pone.0021931
32. El-Hachem N, Haibe-Kains B, Khalil A, Kobeissy FH, Nemer G. AutoDock and AutoDockTools for Protein-Ligand Docking: beta-Site Amyloid Precursor Protein Cleaving Enzyme 1(BACE1) as a Case Study. *Methods Mol Biol*. 2017;1598:391–403. doi:10.1007/978-1-4939-6952-4\_20
33. Liu S, Wang R, Lou Y, Liu J. Uncovering the Mechanism of the Effects of Pien-Tze-Huang on Liver Cancer Using Network Pharmacology and Molecular Docking. *Evid Based Complement Alternat Med*. 2020;2020:4863015. doi:10.1155/2020/4863015
34. Sagoo MK, Gnudi L. Diabetic Nephropathy: an Overview. *Methods Mol Biol*. 2020;2067:3–7. doi:10.1007/978-1-4939-9841-8\_1
35. Sopian S, Budin SB, Taib IS, Mariappan V, Zainalabidin S, Chin KY. Role of Polyphenol in Regulating Oxidative Stress, Inflammation, Fibrosis, and Apoptosis in Diabetic Nephropathy. *Endocr Metab Immune Disord Drug Targets*. 2022;22(5):453–470. doi:10.2174/1871530321666211119144309
36. Wu XQ, Zhang DD, Wang YN, Tan YQ, Yu XY, Zhao YY. AGE/RAGE in diabetic kidney disease and ageing kidney. *Free Radic Biol Med*. 2021;171:260–271. doi:10.1016/j.freeradbiomed.2021.05.025
37. Tóbon-Velasco JC, Cuevas E, Torres-Ramos MA. Receptor for AGEs (RAGE) as mediator of NF- $\kappa$ B pathway activation in neuroinflammation and oxidative stress. *CNS Neurol Disord Drug Targets*. 2014;13(9):1615–1626. doi:10.2174/1871527313666140806144831
38. Su WY, Li Y, Chen X, et al. Ginsenoside Rh1 Improves Type 2 Diabetic Nephropathy through AMPK/PI3K/Akt-Mediated Inflammation and Apoptosis Signaling Pathway. *Am J Chin Med*. 2021;49(5):1215–1233. doi:10.1142/S0192415X21500580
39. Al Mamun A, Ara Mimi A, Wu Y, et al. Pyroptosis in diabetic nephropathy. *Int j Clin Chem*. 2021;523:131–143. doi:10.1016/j.cca.2021.09.003
40. Zhang SZ, Qiu XJ, Dong SS, et al. MicroRNA-770-5p is involved in the development of diabetic nephropathy through regulating podocyte apoptosis by targeting TP53 regulated inhibitor of apoptosis 1. *Eur Rev Med Pharmacol Sci*. 2019;23(3):1248–1256. doi:10.26355/eurrev\_201902\_17018
41. Seok SJ, Lee ES, Kim GT, et al. Blockade of CCL2/CCR2 signalling ameliorates diabetic nephropathy in db/db mice. *Nephrol Dial Transplant*. 2013;28(7):1700–1710.
42. Lenoir O, Gaillard F, Lazareth H, Robin B, Tharaux PL. Hmox1 Deficiency Sensitizes Mice to Peroxynitrite Formation and Diabetic Glomerular Microvascular Injuries. *J Diabetes Res*. 2017;2017:9603924. doi:10.1155/2017/9603924
43. Chen S, Chen L, Jiang H. Prognosis and risk factors of chronic kidney disease progression in patients with diabetic kidney disease and non-diabetic kidney disease: a prospective cohort CKD-ROUTE study. *Renal Failure*. 2022;44(1):1309–1318. doi:10.1080/0886022X.2022.2106872
44. Yonemoto S, Machiguchi T, Nomura K, Minakata T, Nanno M, Yoshida H. Correlations of tissue macrophages and cytoskeletal protein expression with renal fibrosis in patients with diabetes mellitus. *Clin Exper Nephrol*. 2006;10(3):186–192. doi:10.1007/s10157-006-0426-7
45. Nagai K. Dysfunction of natural killer cells in end-stage kidney disease on hemodialysis. *Ren Replace Ther*. 2021;7(1):8. doi:10.1186/s41100-021-00324-0
46. Huang WJ, Liu WJ, Xiao YH, et al. Tripterygium and its extracts for diabetic nephropathy: efficacy and pharmacological mechanisms. *Biomed Pharmacother*. 2020;121:109599. doi:10.1016/j.biopha.2019.109599
47. Tu Q, Li Y, Jin J, Jiang X, Ren Y, He Q. Curcumin alleviates diabetic nephropathy via inhibiting podocyte mesenchymal transdifferentiation and inducing autophagy in rats and MPC5 cells. *Pharm Biol*. 2019;57(1):778–786. doi:10.1080/13880209.2019.1688843
48. Wu X, Li H, Wan Z, et al. The combination of ursolic acid and empagliflozin relieves diabetic nephropathy by reducing inflammation, oxidative stress and renal fibrosis. *Biomed Pharmacother*. 2021;144:112267. doi:10.1016/j.biopha.2021.112267
49. Hu T, Yue J, Tang Q, et al. The effect of quercetin on diabetic nephropathy (DN): a systematic review and meta-analysis of animal studies. *Food Funct*. 2022;13(9):4789–4803. doi:10.1039/d1fo03958j
50. Zhang P, Fang J, Zhang J, Ding S, Gan D. Curcumin Inhibited Podocyte Cell Apoptosis and Accelerated Cell Autophagy in Diabetic Nephropathy via Regulating Beclin1/UVRAG/Bcl2. *Diabetes Metab Syndr Obes*. 2020;13:641–652. doi:10.2147/DMSO.S237451
51. Liu Y, Li Y, Xu L, et al. Quercetin Attenuates Podocyte Apoptosis of Diabetic Nephropathy Through Targeting EGFR Signaling. *Front Pharmacol*. 2021;12:792777. doi:10.3389/fphar.2021.792777
52. Wu W, Wang Y, Li H, Chen H, Shen J. Buyang Huanwu Decoction protects against STZ-induced diabetic nephropathy by inhibiting TGF- $\beta$ /Smad3 signaling-mediated renal fibrosis and inflammation. *ChinMed*. 2021;16(1):118. doi:10.1186/s13020-021-00531-1
53. Luo TT, Lu Y, Yan SK, Xiao X, Rong XL, Guo J. Network Pharmacology in Research of Chinese Medicine Formula: methodology, Application and Prospective. *Chin J Integr Med*. 2020;26(1):72–80. doi:10.1007/s11655-019-3064-0
54. Liu C, Zhang C, He T, et al. Study on potential toxic material base and mechanisms of hepatotoxicity induced by *Dysosma versipellis* based on toxicological evidence chain (TEC) concept. *Ecotoxicol Environ Saf*. 2020;190:110073. doi:10.1016/j.ecoenv.2019.110073

## Diabetes, Metabolic Syndrome and Obesity

Dovepress

### Publish your work in this journal

Diabetes, Metabolic Syndrome and Obesity is an international, peer-reviewed open-access journal committed to the rapid publication of the latest laboratory and clinical findings in the fields of diabetes, metabolic syndrome and obesity research. Original research, review, case reports, hypothesis formation, expert opinion and commentaries are all considered for publication. The manuscript management system is completely online and includes a very quick and fair peer-review system, which is all easy to use. Visit <http://www.dovepress.com/testimonials.php> to read real quotes from published authors.

Submit your manuscript here: <https://www.dovepress.com/diabetes-metabolic-syndrome-and-obesity-journal>